J Mol Model (2011) 17:2237–2248
DOI 10.1007/s00894-010-0949-4

ORIGINAL PAPER

On possible existence of pseudobinary mixed valence fluorides of Ag(I) / Ag(II): a DFT study

Wojciech Grochala

Received: 15 September 2010 / Accepted: 29 December 2010 / Published online: 22 January 2011

Abstract The DFT calculations performed within local density approximation disclose conceivable existence of two novel mixed–valence Ag(I)/Ag(II) fluorides, Ag_2F_3, *i.e.*, Ag(I)Ag(II)F_3 and Ag_3F_4, *i.e.*, Ag(I)$_2$Ag(II)F_4. Ag_2F_3 is predicted to crystallize in three equally stable $NaCuF_3$–, $KAgF_3$–, or $CuTeO_3$–type structures, while Ag_3F_4 should be isostructural to Na_2CuF_4. The calculated vibration-corrected energies of formation at 0 K of Ag_2F_3 and Ag_3F_4 (in their most stable polytypes) from binary fluorides are negative but small (respectively, –0.09 eV and –0.21 eV per formula unit). Formation of Ag_3F_5 (which, in fact, is a mixed valence Ag(I)/Ag(III) salt) from binary fluorides is much less likely, since the energy of formation is quite positive of about a quarter eV. The predicted volumes per formula unit for all forms of Ag_2F_3 are larger and that for K_2CuF_4–type Ag_3F_4 is smaller than the sum of volumes of the corresponding binary fluorides; Ag_2F_3 should not form at high pressure conditions due to a decomposition to the binary constituents. Ag_2F_3 and Ag_3F_4 should exhibit genuine mixed– and not intermediate–valence with quite different coordination spheres of Ag(I) and Ag(II). Nevertheless, they should not be electric insulators. Ag_2F_3 is predicted to be a metallic ferrimagnet with a magnetic superexchange coupling constant, J, of –2 meV while Ag_3F_4 should be a metallic ferromagnet with J of +52 meV. Since Ag_2F_3 and Ag_3F_4 are at the verge of thermodynamic stability, a handful of exothermic reactions have been proposed which could yield these as yet unknown compounds.

Keywords Band theory · Density functional theory · Fluorine · Mixed valence · Oxidizers · Phonons · Silver

This work is dedicated to eminent crystallographer and good friend, Michał Ksawery Cyrański, on his birthday

W. Grochala
ICM, University of Warsaw,
Pawinskiego 5a,
02106 Warsaw, Poland

W. Grochala (✉)
Faculty of Chemistry, University of Warsaw,
Pasteur 1,
02093 Warsaw, Poland
e-mail: wg22@cornell.edu

Introduction: why to search for mixed valence?

Mixed valence compounds constitute a fascinating and quite large family of solids synthesized in the laboratories but also occurring in nature, as exemplified by mineral magnetite Fe(II)Fe(III)$_2O_4$ (archetypical magnet). The very existence of mixed valences within one solid phase is linked to the classical philosophical dilemma of 'Buridan's ass' (Fig. 1): will the valences be mixed, indeed, *i.e.*, trapped at two crystallographically distinct sites (which cannot easily interconvert [1]) or rather will they exhibit an intermediate (*i.e.*, averaged) valence? In the late 1960s Robin and Day have presented a valuable classification of mixed-valence compounds [2] where a division to three distinct groups was proposed. The response to the 'mixed-or-intermediate?' question has been provided by simple but quantitative two-parabola models such as the one by Marcus [3], or the later substantially extended one [4]. Depending on the size of the model parameters (electronic mixing, vibronic mixing, force constant for bond stretching [5]) mixed valence compounds exhibit distinctly different electronic transport and magnetic properties as well as optical absorption spectra. Many of them, such as for example hole- or electron-doped copper oxides [6], show superconductivity.

Silver is no different from other transition metals and it may adopt mixed valence; the following compounds with

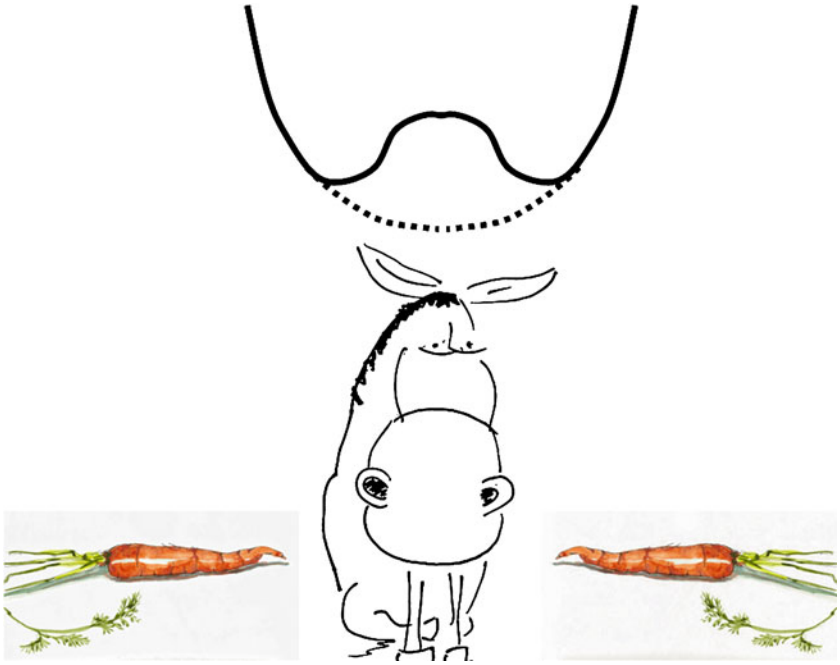

Fig. 1 Illustration of the perpetual 'Buridan's ass' dilemma of chemical compounds with an element at two different formal oxidation states: will they adopt a mixed valence (Robin & Day class I, localized, solid potential energy curve) or rather an intermediate one (Robin & Day class III, delocalized, dotted potential energy curve)? Mixed valence compound offer one more possibility: a fluctuating valence (Robin & Day class II). Buridan's paradox' of medieval logic concerns the dilemma of an ass who is placed equidistantly from two piles of food of equal size and quality in a perfectly symmetrical situation. If the behavior of the ass is completely rational, it will have no reason to prefer one pile to the other and therefore cannot reach a decision over which pile to eat first, so it remains in its original position and starves

Ag at the two different oxidation states have been synthesized in the past (Table 1):

(i) 0 and +1 for Ag_2F [7] and $Ag_2Ni(III)O_2$ [8, 9];
(ii) +1 and +2 for $[Ag(II)(tmc)(BF_4)][Ag(I)_6(C_2)(CF_3CO_2)_5(H_2O)] \cdot H_2O$ (where tmc=1,4,8,11-tetramethyl-1,4,8,11-tetraazacyclotetradecane) [10], fluorosulfate $Ag(I)_2Ag(II)(SO_3F)_4$ [11, 12], $Ag(I)_2Ag(II)(SbF_6)_4$ [13], Ag_9F_{16}, *i.e.*, $Ag(I)_2Ag(II)_7F_{16}$ has been mentioned but its synthesis was never confirmed (Bartlett N (2001) private correspondence)
(iii) +1 and +3 for β–AgF_2 [14], $Ag(I)Ag(III)O_2$ [15] and $Ag(I)_2(Ag(III)_5O_8)L$ where L=NO_3, HF_2 etc. [16]
(iv) +2 and +3 for Ag_3O_4 [17], Ag_2F_5 (*i.e.* $Ag(II)F[Ag(III)F_4]$) [18, 19], Ag_3F_8 (*i.e.*, $Ag(II)[Ag(III)F_4]_2$) [18] and Ag_3MF_{12}, *i.e.*, $\{[Ag(II)F]^+\}_2$ $[Ag(III)F_4^-]$ $[MF_6^-]$ (where M=Au, Pt, Ru, As, Sb) [14].

It is interesting to note that crystal environment of silver cations at two distinct formal oxidation states considerably differs for nearly all compounds listed above, which leads to a mixed- (class I) and not intermediate-valence, with metallic Ag_2F and Ag_2NiO_2 as exclusive exceptions from this rule.

Fluorides of divalent silver are an intriguing class of compounds [20], since they show substantially covalent Ag–F bonding [21] despite a rather low oxidation state of the transition metal. Metallic conductivity has been suggested for salts exhibiting infinite $[AgF^+]$ cations [22] as well as for related $KAgF_3$ [23] and even superconductivity

Table 1 The less known 20 mixed- or intermediate-valence compounds of silver at two various oxidation states, N

N	0	+1	+2	+3
0	X	Ag_2F, Ag_2NiO_2	not known	not known
+1	X	X	$[Ag(tmc^*)(BF_4)][Ag_6(C_2)(CF_3CO_2)_5(H_2O)] \cdot H_2O$, $Ag_3(SO_3F)_4$, $Ag_3(SbF_6)_4$, Ag_9F_{16} (?)	β–AgF_2, Ag_2O_2, $Ag(I)_2(Ag(III)_5O_8)L$ (L=NO_3, HF_2, BF_4, F)
+2	X	X	X	Ag_3O_4, Ag_2F_5, Ag_3F_8, Ag_3MF_{12} (M=Au, Pt, Ru, As, Sb)

* tmc=1,4,8,11-tetramethyl-1,4,8,11-tetraazacyclotetradecane

has been claimed [24] for the Be-Ag-F system with an unknown impurity (likely with O and H traces). Indeed, it has been claimed earlier that properly crystal–engineered fluorides of Ag(II) might exhibit superconductivity [20, 25, 26]. Mixed valence fluoroargentates(II) would thus constitute a valuable extension of the solid state chemistry of Ag(II) and Ag(I) cations, which should be analogous to electron-doped, *i.e.*, Cu(II)/Cu(I) oxide superconductors such as $Nd_{2-x}Ce_xCuO_4$ [27]. They might also allow the formation of the first intermediate valence Ag^{n+} fluoride, where $1<n<2$. This formation could be spontaneous or via chemical doping or high-pressure metallization [28], with concomitant consequences for the electronic transport. At last but not least, Ag_3F_5, Ag_2F_3 and Ag_3F_4 would enrich the spectrum of known fluorides of silver: Ag_2F, AgF, AgF_2, AgF_3, Ag_2F_5, and Ag_3F_8.

Methodology

Computational details

Results presented in this study are based on solid-state calculations done within the density functional theory (DFT) framework using the projector-augmented wave method (PAW) [29] as implemented in the Vienna *ab initio* simulation package (VASP, ver. 4.6 [30–32]). For the exchange-correlation part of the Hamiltonian, the local density approximation (LDA) with the Vosko-Wilk-Nusair exchange–correlation functional [33] has been applied. Full geometry optimization was performed with the SCF convergence criterion set to 10^{-7} eV. The ionic relaxation was continued until the forces on individual atoms were less than 1 meV $Å^{-1}$. The spacing between the k-points for the k-point mesh generation was typically 0.45 $Å^{-1}$ or denser. The valence electrons of highly electronegative fluorine as well as silver at high oxidation states were described by plane waves with a kinetic energy cutoff of 800 eV which provided excellent convergence of total energy of less than 1 meV/atom.

Compounds of Ag(II) with a $4d^9$ electronic configuration are paramagnetic and they often show peculiar magnetism [34]. However, we have observed that allowing for spin polarization does not lead to remarkable modifications of structural features or the energy of polymorphs studied here (similarly to our earlier results for $Ag(II)SO_4$ and $Ag(II)F_2$ [35, 36]); this can be understood if one recalls that magnetic coupling usually constitutes a very small contribution to the electronic energy. This is especially true for compounds containing Ag(II) cation with its single unpaired valence electron; magnetic coupling is usually very weak for such systems and it comes with negligible effect on crystal structure as well as total energy (up to 0.05 eV per one paramagnetic center). As a consequence, results of all *structural* optimizations come from non-spin-polarized LDA calculations.

The *electronic* structure was calculated using both the LSDA and LSDA+U methods with $U(Ag_{4d})=U(F_{2p})=4$ eV, and J=1 eV for both elements (parameters were taken from the previous theoretical study for fluoroargentates(II) [37]). The Dudarev's formalism for U was applied [38]. Magnetic cells were constructed for the following supercells: (1 x 1 x 1) for α–Ag_2F_3 (Z=4), $(\sqrt{2}x\sqrt{2}x1)$ for β– and γ–Ag_2F_3 and for α–Ag_3F_4 (Z=8), (2 x 1 x 1) for β–Ag_3F_4 (Z=4), and later symmetrized to monoclinic (or triclinic, for α–Ag_2F_3) magnetic cells (Z=4 for all polymorphs). The sign of the magnetic superexchange (antiferromagnetic or ferromagnetic, intra-sheet, intra-chain, inter-chain or inter-sheet) for Ag_2F_3 was initially guessed from orbital criteria for the occurrence of magnetism and later confirmed by the calculations of the magnetic superexchange constant J through probing various spin ordering topologies. Due to the presence of low-spin Ag(III) and closed-shell Ag(I), α–Ag_3F_5 will be diamagnetic, and thus no spin-polarized calculations were done.

The resource- and time-demanding calculations of the full phonon dispersion were not performed; instead, phonon frequencies at the center of the first Brillouin zone (Γ) were calculated using VASP. Numerical values for all extensive properties are given per formulae unit (FU) of each compound. Typically, the most stable structures are discussed in this work.

Structural models considered

The energy landscape of a solid with a given stoichiometry may in principle be very complex, so a multitude of chemically reasonable minima should be probed if no experimental structural data is available. The strategy of obtaining the dynamically stable structures used here relies on chemical intuition as well as on selection of starting structures which have a reasonable chance to be isostructural to the studied one. It is important that structural leitmotifs observed for the fluorides of Ag(II) are very similar to those for Cu(II) fluorides, with many known examples of isostructural or structurally tightly–related compounds (Cs_2AgF_4 [39], Rb_2AgF_4 [40] and α–K_2AgF_4 [37] *vs.* K_2CuF_4 [41], β–K_2AgF_4 [42] *vs.* Na_2CuF_4 [43], $KAgF_3$ [37] *vs.* $KCuF_3$ [44, 45] etc.). In consequence, we have tested the following structural models:

(i) For Ag_2F_3: Pbnm $KAgF_3$-type [37], Pmcn $CuTeO_3$-type [46], P-1 $NaCuF_3$- or $AgCuF_3$-type [47, 48], $C222_1$ $BaVS_3$-type [49]

(ii) For Ag_3F_4: $P2_1/c$ β–K_2AgF_4- vel Na_2CuF_4-type [42, 43], Cmca α–K_2AgF_4-type [37], and I4mmm Nd_2CuO_4-type [50]

(iii) For Ag_3F_5: for this rare stoichiometry, we have used P4mbm a defected-K_2RbPdF_5-type with Rb atoms removed [51], Imma $CsPd_2F_5$-type [52], $P2_1/n$ $CsCu_2F_5$-type [53], and I4mmm disordered α–$CsSn_2F_5$-type with one kind of fluoride anions enforced into a special (½ ½ 0) crystallographic position to obtain ordering on anionic sites (which is necessary to perform extended DFT calculations) [54]. Rb_2AgF_5 has been claimed but, regretfully, its crystal structure is not known [55].

The coordination sphere of silver was chemically meaningful for all polymorphs studied (*i.e.*, octahedral or square–planar for Ag(II), linear, octahedral, pseudo-cubic or even one with a larger coordination number for Ag(I)). To assure dynamic stability for each structural type studied, we were following vectors of these normal vibrational modes which exhibited imaginary frequencies in the calculated phonon spectra, until those imaginary modes have disappeared. This approach has been applied in the past to predict the as yet unknown fluorides Au(I)F [56], XeAuF [57] etc.

Building structural models for various fluorides of silver one might consider disproportionation of 2 Ag(II) to Ag(I)+Ag(III). For example, $Ag(I)Ag(II)F_3$ is equivalent to $Ag(I)_{1.5}Ag(III)_{0.5}F_3 \equiv Ag(I)_3Ag(III)F_6$ while Ag_3F_5 to $[Ag(I)_2F][Ag(III)F_4]$ as far as stoichiometry is considered. Coexistence of Ag(I) and Ag(III) is seldom achieved [14] since Ag(III) (either low- or high-spin) is stabilized only in a very basic environment, as for example in $KAgF_4$ [58] or Cs_2KAgF_6 elpasolite [55]. Our previous calculations for $Ag(I)Ag(III)F_4$, (*i.e.*, a disproportionated β form of $Ag(II)F_2$) [36] have shown that disproportionation of Ag(II) in a fluoride environment is slightly thermodynamically disfavored, in contrast to simple oxides (for example, $Ag(I)Ag(III)O_2$ is a stable disproportionated form of a hypothetical Ag(II)O [59]). As will be shown in the next section, the lowest energy polymorph of Ag_3F_5 has a formulation as $[Ag(I)_2F][Ag(III)F_4]$.

The lowest energy polymorphs of Ag_3F_5, Ag_2F_3 and Ag_3F_4

Crystal structures

Let us first discuss aspects of crystal structures, topology and chemical bonding of the lowest energy polymorphs of three hypothetical fluorides of silver; the data regarding the predicted unit cells are contained in Tables 2 and 3.

The lowest energy polymorph of **Ag_3F_5** (from now on as α form) found is tetragonal, of the defected-K_2RbPdF_5-type (P4/mbm, Fig. 2A). Its crystal structure is composed of the alternating $[Ag_2F]_2$ and $[AgF_4]$ layers. Coordination of $[AgF_4]$ units is square planar with four identical Ag–F bonds at 1.999 Å; the very short bond lengths, atypical for Ag(II), suggest the presence of Ag(III). The planes of the neighboring $[Ag(III)F_4^-]$ anions are perpendicular to one another. Ag(I) is coordinated by eight fluoride anions (CN=8) with two 2.249 Å, two 2.268 Å and four 2.570 Å separations. Ag_3F_5 thus resembles structurally to some extent $Ag(I)Ag(III)F_4$ (*i.e.*, a disproportionated β form of $Ag(II)F_2$) [14, 36].

Table 2 The calculated lattice parameters for a few intermediate-valence compounds of silver. Lattice constants for β– and γ–Ag_2F_3 are listed for standard Pnma settings

Compound	a /Å	b /Å	c /Å	α /°	β /°	γ /°
α–Ag_3F_5*	6.089	6.089	6.272	90	90	90
α–Ag_2F_3	5.397	5.882	8.569	90.05	90.96	89.99
β–Ag_2F_3	5.881	8.418	5.506	90	90	90
γ–Ag_2F_3	6.171	8.071	5.291	90	90	90
α–Ag_3F_4	5.526	10.651	6.466	90	90	90
β–Ag_3F_4	3.514	9.179	5.708	90	90.01	90

Three nearly energy-equivalent polymorphs of $AgAgF_3$ of similar topology have been found during theoretical scrutiny. The first one, triclinic (P–1), hereafter referred to as **α–$AgAgF_3$** ($NaCuF_3$–type, Fig. 2B) is a distorted perovskite type, pseudo-orthorhombic and closely related to orthorhombic **β–$AgAgF_3$** (see below). There are two non-equivalent Ag(II) centers in the structure. Both Ag(II) cations adopt a 2+2+2 coordination which resembles an elongated octahedron (I: 2x2.141 Å, 2x2.162 Å, 2x2.461 Å, *i.e.*, 2.255 Å on average; II: 2x2.084 Å, 2x2.106 Å, 2x2.535 Å, *i.e.* 2.242 Å on average). The first coordination sphere of Ag(I) is in the form of a distorted trigonal bipyramide (CN=6, bond lengths 2.211 Å, 2.230 Å, 2.248 Å, 2.404 Å, 2.485 Å, 2.529 Å, with average distance of 2.351 Å) as far as all separations below 2.60 Å are considered. The $[Ag(II)F_6]$ octahedra share the corners; the puckered $[AgF_2]$ sheets separated by [AgF] layers may be distinguished in the crystal structure of this compound. Half of the $[AgF_6]$ octahedra are elongated in the direction more-less perpendicular and another half in the direction parallel to the $[AgF_2]$ sheets, rendering α–$AgAgF_3$ a unique structure.

β–$AgAgF_3$ is closely related to the α form. It is a classic case of the orthorhombically distorted ABF_3 perovskite where too small size of the 12-coordinated B cation leads to the tilting of the $[AF_6]$ octahedra [60] (Fig. 2C). β–$AgAgF_3$ adopts a Pbnm cell ($KAgF_3$-type) with a 2+2+2 coordination of Ag(II) which is not far from an elongated octahedron (2x2.143 Å, 2x2.194 Å, 2x2.477 Å). The first coordination sphere of Ag(I) is in the form of a distorted

Table 3 The formation energies, ΔE_f, for five different mixed valence fluorides of silver as calculated using the LDA method. The truncated (to Γ) zero point energy corrections, $\Delta ZPE_f(\Gamma)$, and the resulting ZPE-corrected formation energies, are also given. ND=not determined

Compound	α–Ag_3F_5	α–Ag_2F_3	β–Ag_2F_3	γ–Ag_2F_3	β–Ag_3F_4	α–Ag_3F_4
ΔE_f /eV	+0.27	–0.07	–0.04	–0.03	–0.17	+0.11
$\Delta ZPE_f(\Gamma)$ /eV	ND	–0.015	–0.033	–0.007	–0.038	–0.029
$\Delta E_f+\Delta ZPE_f(\Gamma)$ /eV	ND	–0.09	–0.07	–0.04	–0.21	+0.08

trigonal bipyramide (CN=6, bond lengths 2.152 Å, 2.161 Å, 2x2.352 Å, and 2x2.418 Å with average distance of 2.309 Å). The [Ag(II)F_6] octahedra share the corners yielding the puckered [AgF_2] sheets. It is also very interesting that – in contrast to $KAgF_3$ [37] – the [AgF_6] octahedra are elongated in the direction perpendicular and not parallel to the sheets, thus rendering β–$AgAgF_3$ topologically more similar to the binary AgF_2 and not to ternary $KAgF_3$ [61, 62]. This feature comes from much smaller Lewis basicity of AgF as compared to KF, and has a strong impact on magnetism (see Mixed valence, electronic structure, band gap at the Fermi level and magnetism).

γ–$AgAgF_3$ ($CuTeO_3$–type), orthorhombic and layered like the α and β phases, contains elongated [Ag(II)F_6] octahedra (2.081 Å, 2.143 Å, 2.390 Å) (Fig. 2D). However, the corner-sharing octahedra are now arranged in such a fashion that the Ag(II)–F–Ag(II) bridge is asymmetric, and the long axes of the octahedra are more-or-less within the propagation direction of the [AgF_2] sheets (as seen also for Cs_2AgF_4 or for $KAgF_3$). Coordination sphere of Ag(I) cation resembles a distorted trigonal bipyramide (CN=6) with Ag(I)-F separations of 2x2.254 Å, 2.316 Å, 2.488 Å, and 2x2.639 Å (average distance is 2.432 Å). In this polymorph the Ag(II)–F bonds (2.205 Å on average) are shorter and stronger than for the α (2.242–2.255 Å) and β (2.271 Å) phases. Simultaneously the Ag(I)–F bonds are weaker and longer (2.432 Å on average *vs.* 2.351 Å and 2.309 Å for α and β phases, respectively).

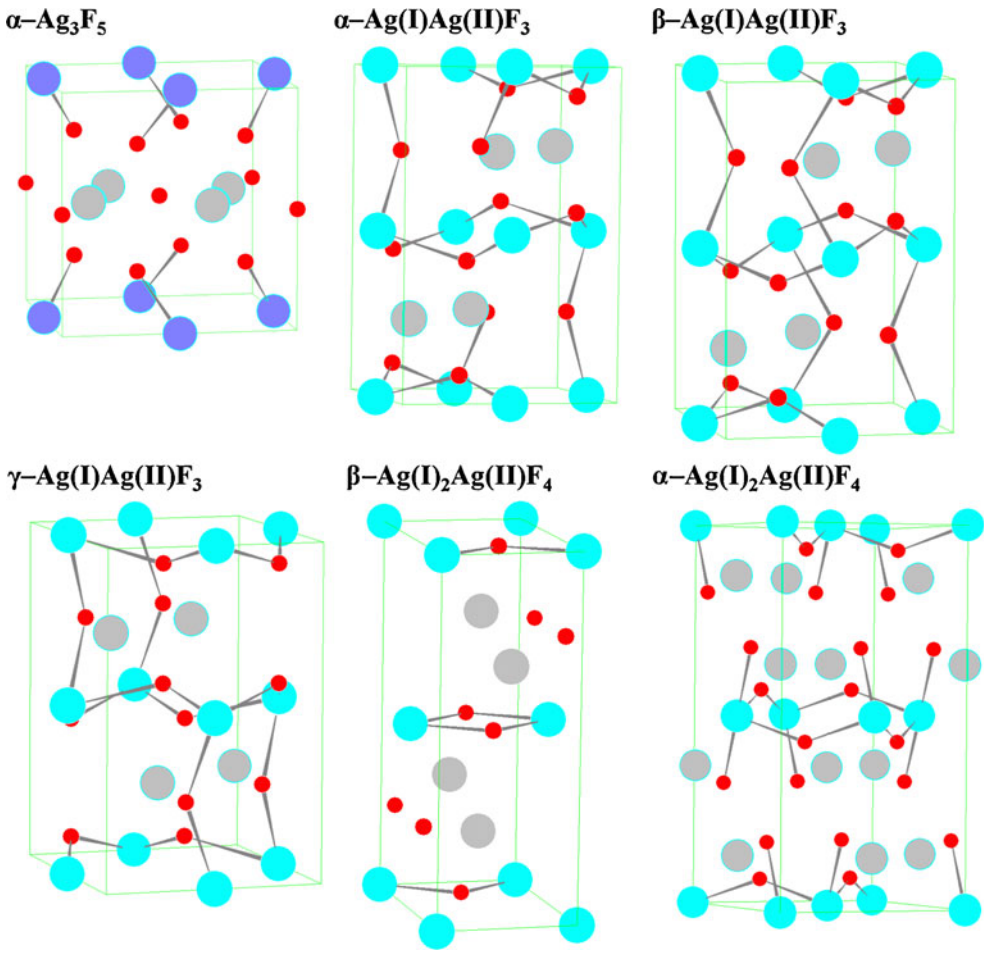

Fig. 2 Illustration of the crystal structures of the most stable polymorphs of Ag_3F_5, Ag_2F_3, and Ag_3F_4. Ag(I) – gray, Ag(II) – blue, Ag(III) – violet, F – red balls

Puckering of the [AgF_2] sheets – as measured by the Ag–F–Ag intra–sheet angles for α, β, and γ forms of Ag_2F_3 (122.6° and 140.1 °, 136.5° and 130.7°, respectively) – is in between those calculated for AgF_2 (117.1°) and $KAgF_3$ (157.3°) (note, the angle of 180° corresponds to flat [AgF_2] sheets). This is consistent with smaller cubic ionic radius of Ag(I) (1.42 Å) as compared to K(I) (1.65 Å).

The most stable form of Ag_3F_4 detected in this work (hereafter referred to as **β–Ag_2AgF_4**) is monoclinic ($P2_1/c$), and analogous to β–K_2AgF_4 and Na_2CuF_4 [42, 43, 63]. This polymorph (Fig. 2E) is characterized by the presence of infinite 1D [$AgF_{4/2}$] chains propagating along the ***a*** crystallographic direction. Coordination of Ag(II) is close to square planar (2x2.193 Å, 2x2.194 Å, <FAgF=73.6°) ([Ag(II)F_4] rectangles share the edges) and thus different from the elongated octahedral one seen for β–K_2AgF_4 [42]. Another important difference between both compounds is that for β–K_2AgF_4 the [AgF_4] plaquettes are perpendicular while for **β–Ag_2AgF_4** they are parallel to the propagation direction of the infinite 1D chains. As we will see, this has important consequences for magnetism (*cf.* Mixed valence, electronic structure, band gap at the Fermi level and magnetism). Ag(I) cations are coordinated by six fluoride ligands (CN=6, bond lengths 4x2.307 Å, 2x2.405 Å with an average distance of 2.340 Å).

Finally, the layered polymorph of Ag_3F_4 considered in this work (**α–Ag_2AgF_4**) is orthorhombic (Cmca), and analogous to α–K_2AgF_4 [37] (Fig. 2F). As expected, this polytype is much less stable from the infinite-chain β–form, due to spatial mismatch of the [AgF_2] and [AgF] sublattices. Coordination of Ag(II) is in the form of a compressed octahedron (2x2.131 Å, 4x2.243 Å, on average 2.206 Å) just like for α–K_2AgF_4 [37]. The first coordination sphere of Ag(I) forms a severely distorted tetrahedron (CN=4, bond lengths 2.180 Å, 2.279 Å, 2x2.327 Å, with average distance of 2.278 Å). The [Ag(II)F_6] octahedra share the corners while forming the puckered [AgF_2] sheets separated by a spacer of two [AgF] layers. Puckering of the [AgF_2] sheets – as measured by the Ag–F–Ag intra–sheet angle of 142.8° – is intermediate between those calculated for AgF_2 (117.1°) and α−K_2AgF_4 (168.0°). Again, this is consistent with smaller cubic ionic radius of Ag(I) as compared to K(I).

Collective Jahn–Teller isomerism

It is intriguing that the three polymorphs of Ag_2F_3 described in the preceding section have virtually identical energy (see Phonons at Γ: indicator of dynamic stability) which may suggest that their crystal topologies (and thus the fashions of how the elongated or compressed [AgF_6] octahedra are interconnected), are equally conceivable. There are three distinct cases (Fig. 3): (a) β–Ag_2F_3 with a short bond–short bond pattern of intra-sheet AgF bonds within the puckered [AgF_2] layers and long inter-sheet AgF bonds, (b) γ–Ag_2F_3 with bond length alternation (short–long) within the puckered [AgF_2] layers and short inter-sheet AgF bonds, and (c) α–Ag_2F_3, an intermediate case between the two with partial bond length alternation within the puckered [AgF_2] layers (*i.e.*, half bonds alternate short–long and another half shows a short-short pattern), and concomitant partial elongation of the inter-sheet AgF bonds (half is long, half is short). Case (a) is analogous to situation incurred for AgF_2, case (b) to $KAgF_3$, while case (c) is unique and has not yet been observed for fluoroargentates(II). The described bond length patterns within [AgF_2] sheets are reflected in the lattice parameters: $b_\beta\,(8.42\text{Å}) \sim c_\alpha(8.57\text{Å}) > b_\gamma\,(8.07\text{Å})$ while $\sqrt{(a_\beta{}^2 + c_\beta{}^2)}\,(6.75\text{Å}) << \sqrt{(a_\alpha{}^2 + b_\alpha{}^2)}\,(7.98\text{Å}) < \sqrt{(a_\gamma{}^2 + c_\gamma{}^2)}\,(8.13\text{Å})$, and in volumes $V_\beta\left(272.6\text{Å}^3\right) > V_\alpha\left(272.0\text{Å}^3\right) > V_\gamma\left(263.5\text{Å}^3\right)$ The uniaxial stress in the direction perpen-

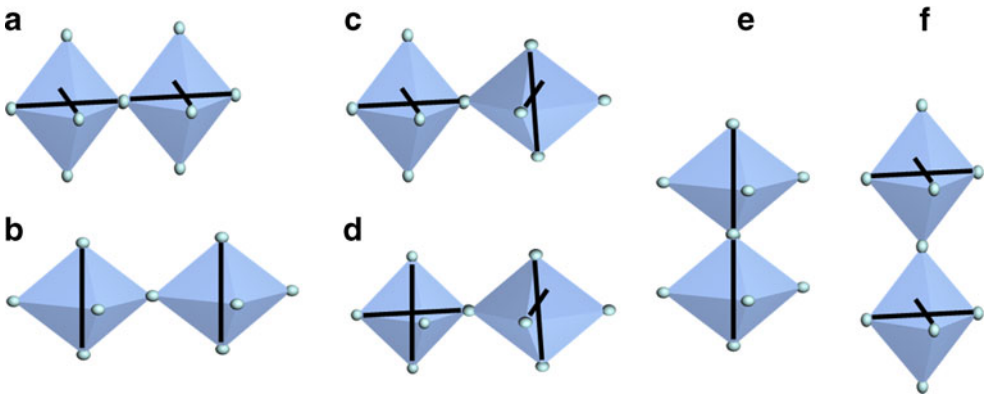

Fig. 3 Illustration of several cases of the collective Jahn–Teller isomerism in fluoroargentates(II). Puckering of the [AgF_2] sheets (due to tilting of the octahedral) was omitted to simplify the picture; short Ag–F bonds are marked in black lines. Cases (**B**) and (**E**) involve compressed octahedra, the remaining cases the elongated ones, and they are exemplified by: (**a**) AgF_2, β–Ag_2F_3, (**b**) α–K_2AgF_4, α–Ag_3F_4, (**c**) α–Ag_2F_3, (**d**) $KAgF_3$, γ–Ag_2F_3, and (**e**) $AgFBF_4$. To our knowledge, so far case (**f**) has not been observed or predicted for any compound of Ag(II)

dicular to the [AgF_2] sheets might thus result in the progressive $\beta \rightarrow \alpha \rightarrow \gamma$ interconversions.

This phenomenon which may be labeled as a "collective Jahn–Teller isomerism", testifies substantial plasticity of the coordination sphere of Ag(II) [64] but it has not yet been observed in experiment for any other fluoroargentate(II) or fluorocuprate (II). It was, however, theoretically anticipated for K_2CuF_4 [65] and for odd-electron Li-Be alloy [66] at elevated pressure.

It is interesting that none of the polymorphs of Ag_2F_3 studied here has a topology related to that of α–K_2AgF_4, with a long bond–long bond pattern within a puckered [AgF_2] sheet (Fig. 3) and short apical AgF distances.

Impact of external pressure on formation and decomposition of mixed–valence fluorides of silver

All mixed valence fluorides studied here have their volumes per FU larger from the sum of volumes of the corresponding binary fluorides. For example, the most stable form of Ag_3F_5 has a volume that is 10.5 $Å^3$ (*i.e.*, 9.9 %) larger than the sum of the volumes of 2 AgF and 1 AgF_2. Similarly, the most stable polymorphs of Ag_2F_3 ($NaCuF_3$-type, $KAgF_3$-type and $CuTeO_3$-type) have the respective differential volumes of +1.28 $Å^3$, 4.47 $Å^3$ and 2.21 $Å^3$ (*i.e.*, 1.9 %, 6.7 % and 3.3 % larger, respectively). β–Ag_3F_4 is an exception with small negative excess volume of –2.4 $Å^3$ per FU (–2.5 %). These results suggest that various forms of the mixed valence Ag_2F_3 are not packed as well as their binary counterparts. Hence they will not form at high pressure conditions (due to decomposition into the binary constituents). Rather, it is advisable to synthesize them at elevated temperature, which usually favors volume expansion. This surmise is analyzed in more detail in "Energetics of formation and impact of temperature".

Phonons at Γ: indicator of dynamic stability

When predicting the possible occurrence of a novel phase or stoichiometry one should address its dynamic stability. It turns out that all phases calculated here do not exhibit imaginary phonon modes at the center of the first Brillouin zone (**Γ**), which suggests their dynamic stability. The truncated (*i.e.*, calculated at **Γ** only) zero-point energy corrections to the formation energies (at T=0 K, see next section) are ranging between –0.015 eV and –0.038 eV, and thus only slightly influence the formation energies (see next section).

Energetics of formation and impact of temperature

While considering the following formation reactions:

$$AgF + 2\,AgF_2 \rightarrow Ag_3F_5 \quad (1)$$

$$AgF + AgF_2 \rightarrow Ag_2F_3 \quad (2)$$

$$2AgF + AgF_2 \rightarrow Ag_3F_4 \quad (3)$$

$$Ag_2F_3 + AgF \rightarrow Ag_3F_4 \quad (4)$$

of mixed valence fluorides of silver with an increasing molar content of AgF (33%, 50%, 67%, respectively), we have calculated the energies of these reactions (Eq. 1–4).

It turns out that the energy of formation of Ag_3F_5 (Eq. 1) is substantially positive, some 0.27 eV per FU. On the other hand, the energies of formation of Ag_2F_3 (Eq. 2) are marginally negative for all three polymorphs (from –0.07 eV to –0.03 eV per FU) while that for β–Ag_3F_4 (Eq. 3) is somewhat more negative (–0.17 eV). The formation energy of Ag_3F_4 from Ag_2F_3 and AgF (Eq. 4) is slightly negative, as well, –0.10 eV, which suggests that β–Ag_3F_4 should be the ultimate product of reaction between AgF_2 and AgF as far as excess of AgF is used. The relatively small negative energy of formation of Ag_2F_3 may be understood considering that formation of mixed-valence fluorides of silver is formally a Lewis acid–Lewis base reaction, for example AgF_2 (acid)+AgF (base)→ $Ag^+[AgF_3^-]$. Since AgF is a weak Lewis base as compared to MF (M=K, Rb, Cs), formation of the $M_{0.5}AgF_{2.5}$, $MAgF_3$ and M_2AgF_4 salts (M=Ag) is not substantially favored. Taking a still different perspective one might say that formation of the mixed-valence systems is connected with the transformation of the lowest-energy 6-coordinated octahedral Ag(I) (in AgF) into either a trigonal bipyramidal, deformed tetrahedral, or 8-coordinated one, which, obviously, comes with an energy increase.

Interestingly, the smaller size of the Ag(I) cation as compared to K(I) results in a relative destabilization of α–Ag_3F_4 by over a quarter eV with respect to the 'collapsed' β–form. Recollect, that for K_2AgF_4 both polymorphs have virtually identical energy as calculated by LDA [42].

Small negative energies of formation for Ag_2F_3 might be supplemented by a favourable entropy term at high temperatures, contributing to thermodynamic stability. An empirical relationship between S° and the volume per FU, V_{FU}, for solid crystalline compounds, proposed by Mallouk and Bartlett [67, 68] was further extended to a wide variety of compounds by Jenkins and Glasser [69]. The correlation takes the form:

$$S^\circ \left[J\,mol^{-1}\,K^{-1}\right] = 1.757\,x V_{FU}\left(Å^3\right) \quad (5)$$

The excess volumes of various polymorphs of Ag_2F_3 as compared to binary substrates, range between 0 and 4.5 $Å^3$,

which translates to 0–7.9 J mol^{-1} K^{-1} in differential entropy of reaction, ΔS^0. The corresponding maximum differential entropy term, [T ΔS^0], is –0.02 eV at 298 K and –0.07 eV at 900 K, thus it is comparable to or even exceeds the energy of formation of all polymorphs of Ag_2F_3, while contributing to their increased thermodynamic stability at elevated temperatures.

Concluding this section we would like to emphasize that it is worth pursuing synthesis of Ag_2F_3 at elevated temperatures. Complete evaluation of thermodynamics of formation of mixed–valence fluorides of silver obviously requires precise resources-demanding calculations of full phonon dispersion and accurate reproduction of the lowest-energy phonon modes, and it is beyond the scope of the current study.

Mixed valence, electronic structure, band gap at the Fermi level and magnetism

Ag(II) has a $4d^9$ electronic configuration and it is paramagnetic. Electronic structure and magnetism of mixed-valence pseudobinary fluorides of silver, are therefore of interest. Will these compounds be metallic or insulating, show wide- or narrow-band gap, be ferro- or antiferromagnetic, similar to binary AgF_2 or rather to ternary potassium fluoroargentates(II)? To answer these questions we have carried out calculations of the electronic band structures and electronic density of states for the most stable forms of Ag_2F_3 and Ag_3F_4 at the LSDA (not shown) and LSDA+U levels (Figs. 4 and 5).

Inspection of the partial density of states shows that the electronic states predominated by 4d functions of Ag(I) cations are quite separated in energy from those of Ag(II) cations for the compounds studied. For example, the former are found in the (–1, 0) eV energy window, while the latter in the (0, +1) eV window for α–Ag(I)Ag(II)F_3. This result is not surprising if we recollect that the coordination spheres of both types of cations were very different for all stoichiometries and polymorphs considered (*cf.* Sect. 3.1). In other words, the mixed valence fluorides of silver described in this work show genuine mixed- and not intermediate-valence. The vertical inter-valence charge transfer (IVCT) optical transitions are predicted to arise

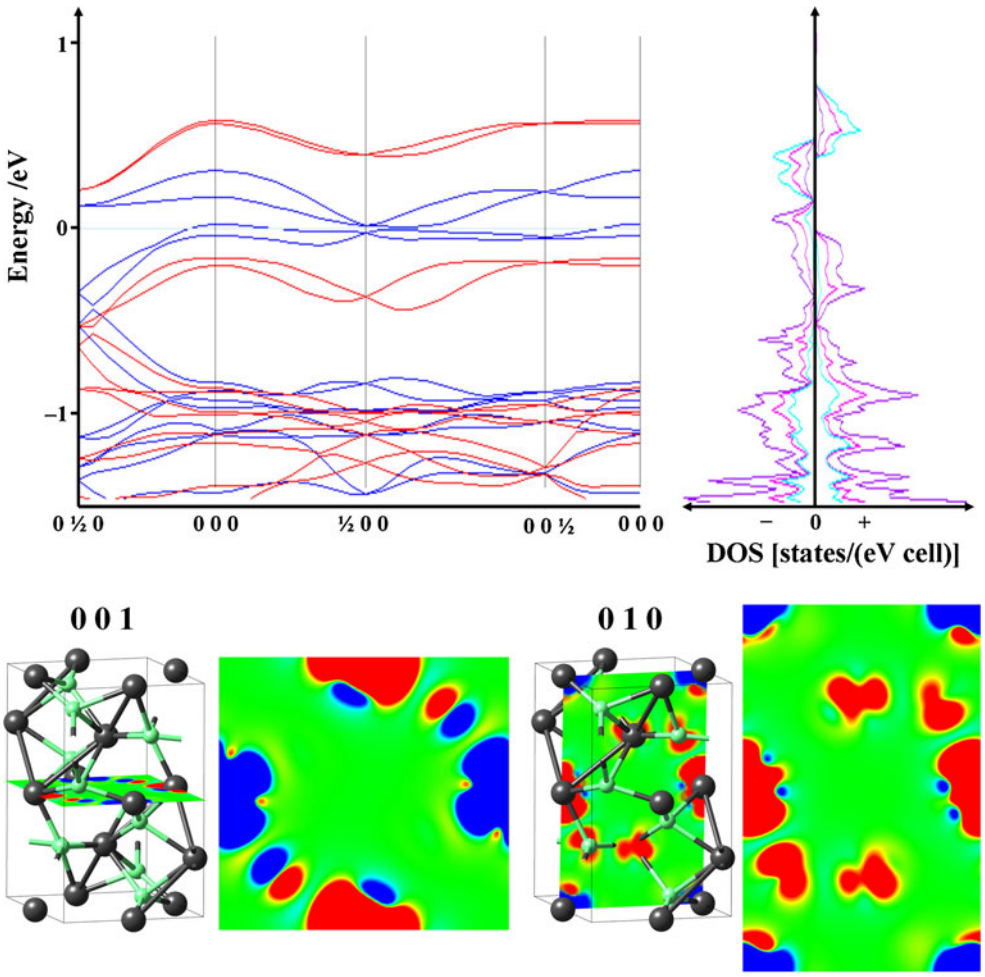

Fig. 4 The electronic band structure (majority spins – red, minority spins – blue) and electronic density of states for the most stable α polymorph of Ag(I)Ag(II)F_3, with atomic contributions from F (rose), Ag(I) (violet) and Ag(II) (ocean blue) as calculated at the LSDA+U level. Projections of spin density (up to 0.01 e $Å^3$) indicating pathways for facile magnetic superexchange, are also shown (blue and red stand for excess and depletion of α density, respectively)

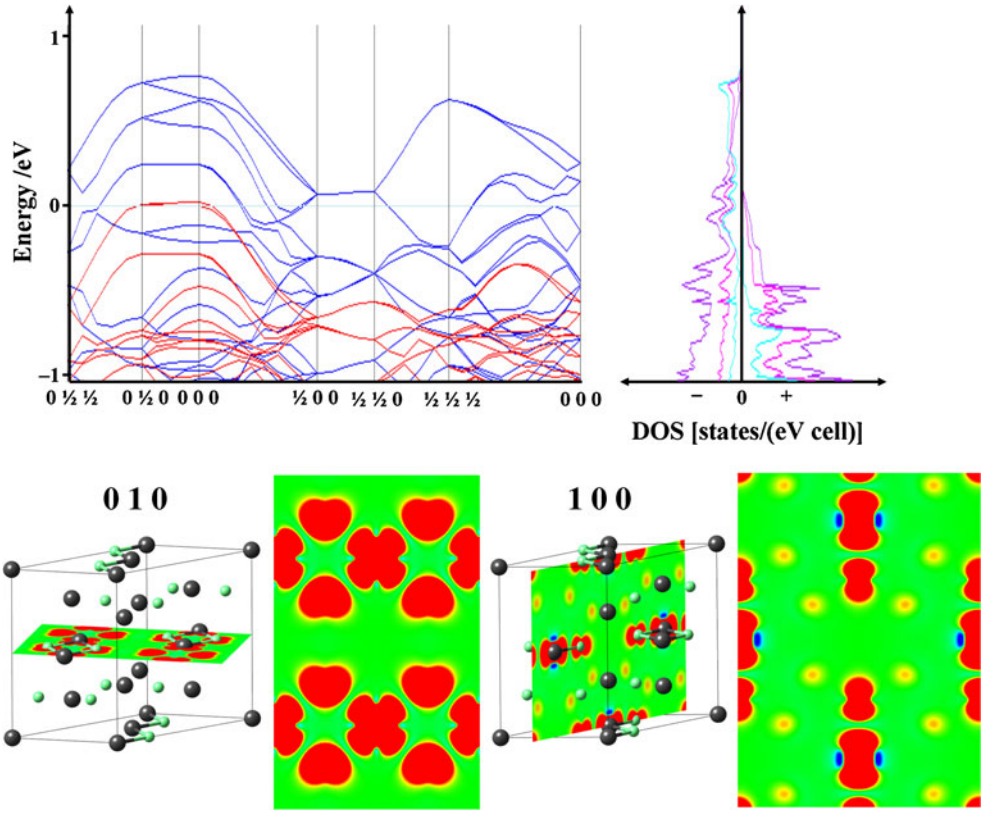

Fig. 5 The electronic band structure (majority spins – red, minority spins – blue) and electronic density of states for the most stable β polymorph of $Ag(I)_2Ag(II)F_4$, with atomic contributions from F (rose), Ag(I) (violet) and Ag(II) (ocean blue) as calculated at the LSDA+U level. Projections of spin density (up to 0.01 e $Å^3$) indicating pathways for facile magnetic superexchange, are also shown (blue and red stand for excess and depletion of α density, respectively)

between the highest occupied Ag(I) states and formally half-empty electron-deficient Ag(II) states; calculations (not taking into account the electron–hole attraction) locate the lowest energy IVCT transitions at less than 1 eV. These compounds should thus appear black to the eye and show metallic luster. All silver states are firmly hybridized with the 2p functions of F, like many others fluorides of silver [20].

It turns out that all structures with artificially enforced antiferromagnetic ordering of spins converge to metallic solutions at the LSDA level. This situation is quite typical for the late transition d^9 systems such as CuF_2 or AgF_2 [70]. Inclusion of the on-site electron repulsion via a Hubbard U term (at the LSDA+U level) stabilizes magnetic solutions but does not open band gaps at the Fermi level (Figs. 4 and 5). Hence, the compounds studied may be labeled as magnetic metals.

All mixed valence fluorides of silver except for α–Ag_3F_4 show the coordination sphere of Ag(II) in the form of a more-or-less elongated octahedron. It is thus expected that magnetic coupling between the $d(x^2–y^2)$ electrons (ferro- or antiferromagnetic in type) will depend only on a mutual orientation of the $[Ag(II)F_4]$ plaquettes. If the Ag–F–Ag angle defining geometry of the fluoride bridge is close to 180°, antiferromagnetism is expected; if it is close to 90°, ferromagnetism should appear. The calculated Ag–F–Ag angle falls between these two values for all compounds studied here. For example, the intra-chain Ag–F–Ag angle ranges from 106.4° for β–Ag_3F_4 (double F bridge, ferromagnetism expected), via 140.1° for α–Ag_2F_3, to 140.6–142.9° for γ–Ag_2F_3 (single F bridge, antiferromagnetism more likely). The intra-sheet Ag–F–Ag angle ranges from 122.6° for α–Ag_2F_3 (ferromagnetism expected) via 130.7° for γ–Ag_2F_3 and 136.5° for β–Ag_2F_3, to 142.8° for α–Ag_3F_4 (antiferromagnetic coupling possibly favored).

The LSDA+U calculations (Table 4) suggest that β–Ag_3F_4 should indeed order ferromagnetically (in one dimension, along the propagation direction of the $[AgF_{4/2}]$ chains) while α–Ag_2F_3 should show 3D magnetism with antiferromagnetic-type both intra- and inter-sheet coupling; due to different magnetic moments on crystallographically independent Ag(II) cations α–Ag_2F_3 should be described as ferrimagnet. The absolute values of the calculated magnetic moments on Ag(II) vary between 0.34 μ_B and 0.44 μ_B and they are smaller than those calculated for AgF_2, $KAgF_3$ and β–K_2AgF_4 (0.51–0.56 μ_B). Those on bridging fluoride anions are in the 0.08–0.11 μ_B range, very close to the value calculated for $KAgF_3$ (0.10 μ_B). As expected, Ag(I) cations carry rather little spin, with magnetic moments of 0.14 μ_B at most.

The approximate value of the magnetic superexchange constant, J, has been calculated from the following expression:

$$J \approx Nx\, \Delta E^{AFM/FM}\,(meV) \qquad (6)$$

Table 4 The values of the intra-sheet or intra-chain (*) magnetic superexchange constant (J /meV) and magnetic moments on Ag(II) and F centers, for five different mixed valence fluorides of silver as calculated using LSDA+U method. Negative and positive sign of J stands for an antiferro- and ferromagnetic coupling, respectively. Values calculated for AgF_2 and $KAgF_3$ are shown for comparison. ND=not determined

Compound	α–Ag_2F_3	β–Ag_3F_4	AgF_2	$KAgF_3$	β–K_2AgF_4
J_{LSDA+U} /meV	–2*	+52**	–4.7***	ND**	ND**
μ(Ag(II)) /μ_B	+0.38, –0.44	+0.34	±0.54	±0.51	±0.56
μ(Ag(I)) /μ_B	+0.03	+0.14	—	—	—
μ(F_{bridge}) /μ_B	+0.09, –0.08	+0.11	0.00	±0.10	+0.10
μ($F_{terminal}$) /μ_B	–0.01	+0.08	—	0.00, ±0.10	+0.10
Reference	This work	This work	[70]	[40]	[42]

* 3D ** intra-chain (1D) *** intra-sheet (2D)

where N=2 for 1D case, N=1 for 2D case, and N=2/3 for 3D case (Table 3). The value of J calculated for α–Ag_2F_3 is –2 meV, less than half of that predicted for AgF_2; although the size of J is not impressive yet the type of magnetic ordering is of interest, rendering α–Ag_2F_3 the first candidate for a 3D fluoroargentate(II) antiferromagnet. On the other hand, J calculated for β–Ag_3F_4 is as large as +52 meV, indicating strong ferromagnetic coupling via a [F_2] bridge. Strong coupling must be due to the short Ag…Ag distance, and favorable value of the Ag–F–Ag (close to 90°). The absolute value of J is still smaller than the giant value of –298 meV predicted for the compressed 2D form of AgF_2 exhibiting flat [AgF_2] sheets [71].

How might one attempt to synthesize Ag_2F_3 and Ag_3F_4?

Conceivable existence of mixed–valence fluorides of silver (I/II) deduced from DFT calculations poses a question how these compounds might be synthesized in the laboratory. β−Ag_3F_4 should be achieved quite easily, for example:

(i) Via prolonged exposure of AgF_2 to ultra-pure argon gas or at dynamic vacuum at temperatures slightly lower than its thermal decomposition temperature of 690 °C;
(ii) Via photochemical decomposition of AgF_2;
(iii) Via electrochemical oxidation of saturated solutions oh $AgHF_2$ in aHF on glassy carbon or platinum electrodes;
(iv) Via high pressure synthesis, due to its more compact crystal structure than those for AgF and AgF_2.

On the other hand, calculations suggest that Ag_2F_3 is close to a thermodynamic equilibrium with a mixture of binary fluorides at 0 K and only slightly stabilized by the entropy term at elevated temperature conditions. It is thus advisable to use reagents capable of yielding exothermic reactions; the following preparative methods are suggested:

(i) Attempts of selective reduction of AgF_2 using C_6F_6, $C_{10}F_8$, C_6Cl_6, Cl_2 or similar poor reducing agents;
(ii) High-energy milling of AgF_2 and AgF in PTFE (Teflon®) mills; please note that local temperature at the intergrain boundary rises considerably when using this method;
(iii) Alternative mechanochemical synthesis utilizing $Ag(SbF_6)$ and $KAgF_3$ or related reagents;
(iv) Methathesis in anhydrous HF between $M_x(SbF_6)$ (or related soluble salts) and excess of AgF (if formation of binary AgF_2 could be prevented (Mazej Z, Grochala W (2008) unpublished results)).

It is of interest if these theoretical predictions could be confirmed by experiments.

Conclusions

Compounds containing silver at mixed valence (I/II) are immensely rare. The DFT calculations described in this work suggest conceivable existence of two novel mixed–valence Ag(I)/Ag(II) fluorides, $Ag_2F_3 \equiv Ag(I)Ag(II)F_3$ and $Ag_3F_4 \equiv Ag(I)_2Ag(II)F_4$, exhibiting crystal structures with

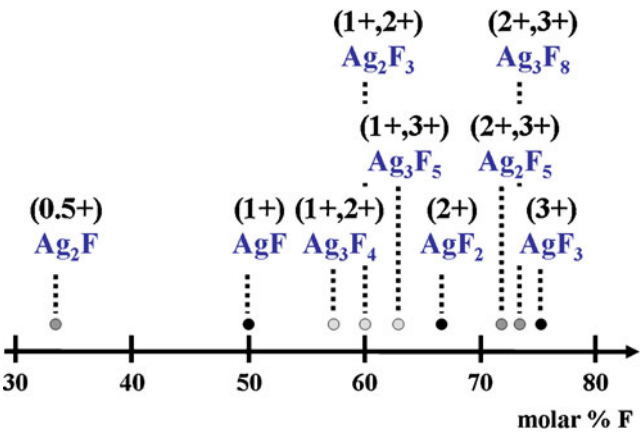

Fig. 6 The known phases appearing in the Ag–F phase diagram together with hypothetical mixed–valence fluorides predicted in this work; molar % F and oxidation state(s) of Ag are shown

puckered [AgF_2] sheets and infinite [$AgF_{4/2}$] chains, respectively. The energies of formation from binary fluorides for the most stable polytypes of the mixed–valence compounds are predicted to be marginally negative, at the positive excess volume for Ag_2F_3 and the negative one for Ag_3F_4. Ag_3F_4 might thus be obtained directly from 2 AgF and AgF_2 but Ag_2F_3 should be searched for either at high T conditions or as a product of various exothermic reactions. Both quasi-binary fluorides should exhibit mixed- and not intermediate valence, be strongly correlated metals, and order magnetically at low temperatures. The predicted intra-chain superexchange coupling constants, J, are –2 and +52 meV for the lowest energy α–Ag_2F_3 and β–Ag_3F_4 polymorphs, respectively. Ag_3F_5 is shown in fact to be a diamagnetic mixed valence Ag(I)/Ag(III) fluoride, $Ag(I)_2Ag(III)F_5$, thermodynamically unstable with respect to AgF / 2 AgF_2 constituents.

A number of viable synthetic pathways are suggested which could help to confirm – or refute – these predictions in experiment. If synthesized, pseudo-binary Ag_2F_3 and Ag_3F_4 would enrich the spectrum of the known fluorides of silver: Ag_2F, AgF, AgF_2, AgF_3, Ag_2F_5, and Ag_3F_8 (Fig. 6).

Acknowledgments The project ‘Quest for superconductivity in crystal-engineered higher fluorides of silver’ is operated within the Foundation for Polish Science ‘TEAM’ Program co-financed by the EU European Regional Development Fund. Calculations have been performed at Interdisciplinary Centre for Mathematical and Computational Modelling (ICM) supercomputers. WG is grateful to ICM and Faculty of Chemistry, University of Warsaw, for financial sustenance.

References

1. Fe_3O_4 mentioned here is actually a more complex case, with Fe (III) cations at the A site of the spinel and both Fe(II) and Fe(III) cations at the B site
2. Robin MB, Day P (1967) Adv inorg chem radiochem 10:247–422
3. Marcus RA (1993) Angew Chem Int Ed Engl 32:1111-1121
4. Barbara PF, Meyer TJ, Ratner MA (1996) J Phys Chem 100: 13148-13168
5. Grochala W, Hoffman R (2000) J Phys Chem A 104:9740-9749 and references therein
6. Bednorz JG, Müller KA (1986) Z Phys B Con Mat 64:189–193
7. Williams A (1989) J Phys Condens Mat 1:2569–2574
8. Yoshida H, Muraoka Y, Sörgel T, Jansen M, Hiroi Z (2006) Phys Rev B 73:020408(R)-1 to -4
9. Schreyer M, Jansen M (2002) Angew Chem Int Ed Engl 41:643–646
10. Wang QM, Lee HK, Mak TCW (2002) New J Chem 26:513–515
11. Leung PC, Aubke F (1978) Inorg Chem 17:1765–1772
12. Michałowski T et al. (2010) 16th European Symposium on Fluorine Chemistry, Ljubljana Slovenia
13. Mazej Z (2010) Pacifichem – The International Chemical Congress of Pacific Basin Societies, Honolulu USA
14. Shen CP, Žemva B, Lucier GM, Graudejus O, Allman JA, Bartlett N (1999) Inorg Chem 38:4570–4577
15. McMillan JA (1960) J Inorg Nucl Chem 13:28–31
16. Robin MB, Andres K, Geballe TH, Kuebler NA, McWhan DB (1966) Phys Rev Lett 17:917–919
17. Standke B, Jansen M (2003) Angew Chem Int Ed Engl 25:77–78
18. Žemva B et al. (1991) J Am Chem Soc 113:4192–4198
19. Kraus M, Müller M, Fischer R, Schmidt R, Koller D, Müller BG (2000) J Fluorine Chem 101:165–171
20. Grochala W, Hoffmann R (2001) Angew Chem Int Ed Engl 40:2743–2781
21. Grochala W, Egdell RG, Edwards PP, Mazej Z, Žemva B (2003) Chem Phys 4:997–1001
22. Lucier GM, Münzenberg J, Casteel WJ, Bartlett N (1995) Inorg Chem 34:2692–2698
23. Grochala W, Edwards PP (2003) Phys Status Solidi B 240:R11–R14
24. Grochala W, Porch A, Edwards PP (2004) Solid State Commun 130:137–142
25. Grochala W (2005) J Mol Model 11:323–329
26. Grochala W (2009) J Mater Chem 19:6949–6968
27. Tokura Y, Tagaki H, Uchida S (1989) Nature 337:345–347
28. Grochala W, Feng J, Hoffmann R, Ashcroft NW (2006) Angew Chem Int Ed Engl 46:3620–3642
29. Blöchl PE (1994) Phys Rev B 50:17953–17979
30. Kresse G, Furthmüller J (1996) Phys Rev B 54:11169–11186
31. Kresse G, Furthmüller J (1996) Comput Mater Sci 6:15–50
32. Kresse G, Joubert D (1999) Phys Rev B 59:1758–1775
33. Vosko SH, Wilk L, Nusair M (1980) Can J Phys 58:1200–1211
34. Malinowski PJ, Derzsi M, Gaweł B, Łasocha W, Jagličić Z, Mazej Z, Grochala W (2010) Angew Chem Int Edit 49:1683–1686
35. Derzsi M, Dymkowski K, Grochala W (2010) Inorg Chem 49:2735–2742
36. Romiszewski J, Stolarczyk L, Grochala W (2007) J Phys Condens Matter 19:116206-1 to -13
37. Mazej Z et al. (2009) Cryst Eng Comm 11:1702–1710
38. Dudarev SL, Botton GA, Savrasov SY, Humphreys CJ, Sutton AP (1998) Phys Rev B 57:1505–1509
39. McLain SE et al. (2006) Nat Mater 5:561–566
40. Kurzydłowski D et al. (2010) 16th European Symposium on Fluorine Chemistry, Ljubljana Slovenia
41. Hidaka M, Inoue K, Yamada I, Walker PJ (1983) Physica B+C 121:343–350
42. Kurzydłowski D et al. (2010) Eur J Inorg Chem 19:2919–2925
43. Babel D (1965) Z Anorg Allg Chem 336:200–206
44. Buttner RH, Maslen EN, Spadaccini N (1990) Acta Crystallogr B 46:131–138
45. Hidaka M, Eguchi T, Yamada I (1998) J Phys Soc Jpn 67:2488–2494
46. Lindqvist O (1971) Acta Chem Scand 25:740–787
47. Kaiser V, Otto M, Binder F, Babel D (1990) Z Anorg Allg Chem 585:93–104
48. Tong J, Lee C, Whangbo MH, Kremer RK, Simon A Köhler J (2010) Z Kristallogr 12:680–684
49. Ghedira M, Anne M, Chenavas J, Marezio M, Sayetat F (1986) J Phys C 19:6489–6503
50. Müllerbuschbaum H, Wollschlager W (1975) Z Anorg Allg Chem 414:76–80
51. Bachmann B, Müller BG (1991) Z Anorg Allg Chem 597:9–18
52. Müller BG (1982) Z Anorg Allg Chem 491:245–252
53. Kaiser V, Babel D (1990) Acta Crystallogr A 46:367–368
54. Berastegui P, Hull S, Eriksson SG (2010) J Solid State Chem 183:373–378
55. Hoppe R, Homann R (1966) Naturwiss 53:501–501
56. Kurzydłowski D, Grochala W (2008) Chem Commun 1073-1075
57. Kurzydłowski D, Grochala W (2008) Z Anorg Allg Chem 634:1082–1086
58. Hoppe R (1957) Z Anorg Allg Chem 292:28–33

59. See Supplementary Information for Ref. [36] for DFT calculations
60. King G, Woodward PM (2010) J Mater Chem 20:5785–5796
61. Fischer P, Schwarzenbach D, Rietveld HM (1971) J Phys Chem Solids 32:543–550
62. Jesih A et al. (1990) Z Anorg Allg Chem 588:77–83
63. The $P2_1/c$ cell is pseudo-orthorhombic ($\beta=90.01^{o}$) and it may be symmetrized to Cmmm; this comes with energy bill of +0.02 eV per FU
64. Grochala W (2006) Phys Statud Solidi B 243:R81–R83
65. Mitrofanov VY, Nikiforov AE, Shashkin SY (1997) Solid State Commun 104:499–504
66. Feng J, Hennig RG, Ashcroft NW, Hoffmann R (2008) Nature 451:445–448
67. Bartlett N, Yeh S, Kourtakis K, Mallouk TE (1984) J Fluorine Chem 26:97–116
68. Shen CS, Hagiwara R, Mallouk TE, Bartlett N (1994) In: Inorganic Fluorine Chemistry Toward the 21st Century. American Chemical Society, Washington DC, p 26
69. Jenkins HDB, Glasser L (2003) Inorg Chem 42:8702–8708
70. Derzsi M, Leszczyński P, Grochala W (2010) unpublished data. Grochala W et al. (2010) 16th European Symposium on Fluorine Chemistry, Ljubljana Slovenia
71. Jaroń T, Grochala W (2008) Phys Status Solidi R 2:71–73